THE ENTRAINMENT INTERFACE LAYER OF STRATOCUMULUS-TOPPED BOUNDARY LAYERS DURING THE POST FIELD CAMPAIGN

Samantha A. Hill,[1] Steven K. Krueger,[1] Hermann Gerber,[2] and Szymon P. Malinowski[3]

[1]University of Utah, Salt Lake City, Utah, USA

[2] Gerber Scientific Inc., Reston, Virginia, USA

[3] University of Warsaw Institute of Geophysics, Warsaw, Poland

1. INTRODUCTION

The fine-scale cloud structure near the top of Stratocumulus-Topped Boundary Layers (STBLs) has remained unexplored for many years due to limitations in aircraft and technology. This cloud top region in marine stratocumulus (Sc) is especially of interest because processes taking place there are believed to govern the behavior and persistence of the cloud decks that form at the top of these boundary layers. Small-scale cloud-top processes influence physical characteristics of these cloud layers, such as albedo, which currently plays a major role in keeping the earth's climate cooler than it would be in their absence due to the high amount of incident solar radiation marine Sc cloud decks reflect back to space (Bretherton 1997; Klein and Hartmann 1993). Thus, marine STBLs play an important role in Earth's radiation balance and climate (Hartmann 1992). Furthermore, studies have shown that uncertainties in the behavior of Sc clouds inhibit the accurate prediction of future climate change (Bony et al. 2006; Wyant et al. 2006). Therefore, largely due to their potential influence on climate, and due to the fact that little is understood about the small-scale processes that influence the behavior of these clouds, STBLs have remained a central topic in cloud physics research.

Our results are based on high-resolution aircraft data from the Physics of Stratocumulus Top (POST) field campaign that took place during July and August of 2008 off the coast of Monterey, California. A major focus of POST was sampling the fine-scale structure of the entrainment interface layer (EIL), the transition layer between the top of the cloudy mixed layer and the free troposphere. Consequently, a major result of our work is an approximation of the location and extent of the EIL for a subset of flights during POST. Using total water mixing ratio and liquid water potential temperature, we calculated the mixing fraction. This quantity is an indicator of the degree of mixing a parcel has undergone. We focused on five research flights during POST: two in the day, and three in the evening. Further, we used a mixing fraction analysis to calculate the warming and cooling due to radiative processes and phase changes near cloud top. For all of the flights analyzed, we find a clearly defined EIL, and that the effects of radiation and phase changes on net heating or cooling within the EIL are comparable. Our results support the idea that entrainment involves a buoyancy-sorting process in which mixtures with various fractions of free-atmosphere and mixed-layer air are produced in the EIL, but only those parcels with neutral or negative buoyancy relative to the mixed layer are entrained.

2. FLIGHT PATHS AND SELECTING DATA

With the EIL being a primary focus of the POST project, vertical flight plans were specially designed to collect data from within the EIL, and from the regions transitioning into, and out of, the EIL. These flightpaths were comprised of three (sometimes four) sections of repeated "sawtoothing" through the cloud deck, meaning the aircraft would dip down into the cloud layer, and then once in the cloud layer, would rise back up above the cloud layer. This pattern was repeated several times within a section of the flight path. Also, level legs were flown near the surface, in-cloud, and just below the cloud layer for later calculation of fluxes. An example of a typical vertical flight path is shown in Figure 1.
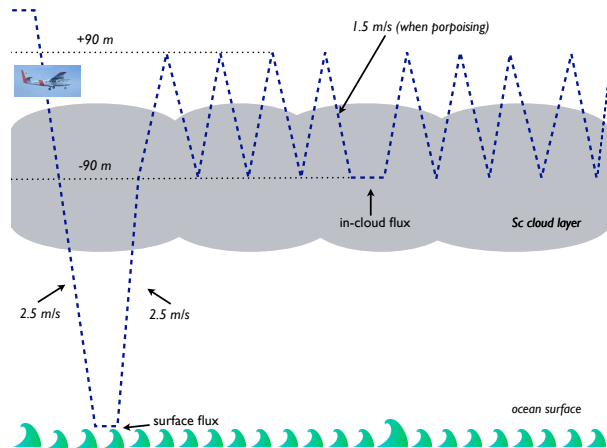
Figure 1: Diagram of a section of a typical vertical flight path during POST.

Figure 2: A typical horizontal flightpath during POST.

Simultaneously, in the horizontal, the flight path was prescribed as well, in an attempt to sample consistent parcels of air. Instead of simply flying down the coast or maintaining a straight path within the Sc layer, the pilot was assigned to fly a quasi-Lagrangian flight path, meaning the aircraft would follow the general flow of the surrounding atmosphere while sampling as much as possible from the same parcel of air, resulting in an overall zig-zag pattern. An example of the horizontal quasi-Lagrangian flight path from Research Flight 10 is shown in Figure 2.

Most of the data collected during POST were gathered by high-rate, fast-response probes at a frequency of 1000 Hz. However, to accommodate LI-COR vapor data, which was taken at a lower frequency of just 40 Hz., the 1000 Hz. data sets were averaged to 40 Hz. using matrix techniques in Matlab. Data from the aircraft cabin instrumentation were used for calculations involving ambient air pressure and height data. As the recording frequency for the cabin instruments was only 10 Hz., these data were interpolated to 40 Hz. using Matlab interpolation functions.

As previously mentioned, each flight included sections of "porpoising" in and out of the cloud layer, as well as horizontal legs for calculating fluxes. The analyses included here mainly focus on studying the extent and structure of the EIL; therefore, they focus on the portions of each flightpath that were comprised of these porpoises, and the data used for these analyses are solely those data points from within the porpoising sections of the flightpath. These groups of repetitive porpoises during each flight were named "pods." In most cases, each flight contained three pods comprised of at least five porpoises each. Most results of the following analyses are in the form of results from pods of a given flight.

3. CONSERVED VARIABLES AND MIXING

The use of conserved variables to investigate mixing between two thermodynamically distinct types of air within clouds has been employed in several studies (Burnet and Brenguier 2007; Paluch 1979). Specifically, this type of analysis has proven useful to study parcels in the midst of entrainment as dry and warm free-tropospheric air mixes with cool and moist cloudy air. Moist conserved variables, such as total water mixing ratio (q_t), are important for these analyses because they are conserved quantities under moist adia-

batic processes, and will remain constant, regardless of the altitude of the parcel in the atmosphere. For two parcels of different types of air undergoing mixing, a conserved variable, such as q_t, of the new mixture will be a linear combination of the q_ts of the original parcels, weighted by the mass contribution of each original parcel to the mass of the resultant mixture:

$$q_{t,mix} = (1 - \chi) * q_{t,a} + \chi * q_{t,b}, \qquad (1)$$

where $q_{t,a}$ is the total water mixing ratio of the first parcel, and $(1-\chi)$ is the fraction of unit mass contributed to the final mixture from the first parcel, while $q_{t,b}$ is the total water mixing ratio of the second parcel, and χ is the fraction of unit mass contributed to the final mixture from the second parcel.

Due to this linear characteristic of mixing for conserved variables, all possible mixing states for a resultant mixture between the initial, distinct states of the two original parcels lie on a straight line connecting a point representing the original mixing state of the first parcel, and a point representing the original mixing state of the second parcel. This is called a mixing line.

For studying mixing near the top of Sc clouds, one pure mixing state is taken to be the cloudy layer at the top of the STBL, and the second pure mixing state is taken to be the free troposphere overlying the STBL. VanZanten and Duynkerke (2002) suggest a method for using a conserved variable called mixing fraction to study radiative and phase change effects on temperature near the top of a Sc layer. Mixing fraction is a measure of the amount of one type of air mixed into a parcel of a second type of air, and is calculated using ratios and differences in q_t for the two types of air.

Locating mixing events at the top of the STBL during POST first required defining pure mixing states in and above the boundary layer. Moist, turbulent, cloud-layer air was defined as one such mixing state, and dry, warm, free-troposphere air from above the inversion was defined as a second pure state. The mixing of these two pure states was then used to study the properties of the EIL.

First, it was necessary to select and use variables that are conserved under both dry adiabatic and moist adiabatic processes due to the presence of moisture in both vapor and liquid phases throughout circulations within the mixed layer. The two moist conserved variables selected for this analysis were q_t (which remains constant though moisture may change from the vapor state to the liquid state, or visa versa), and liquid water potential temperature (Θ_l). An example of a mixing line from one pod of a daytime flight during POST is shown in Figure 3, with density of points expressed via color-coding. In this figure, one can see that most points are located at either endpoint of the mixing line in either one of the pure mixing states, but many parcels are located on the mixing line in between the pure states, in various stages of the mixing process. Data points that have been shifted to the right or left of the mixing line show the effects of radiative heating or cooling on parcels within the EIL.
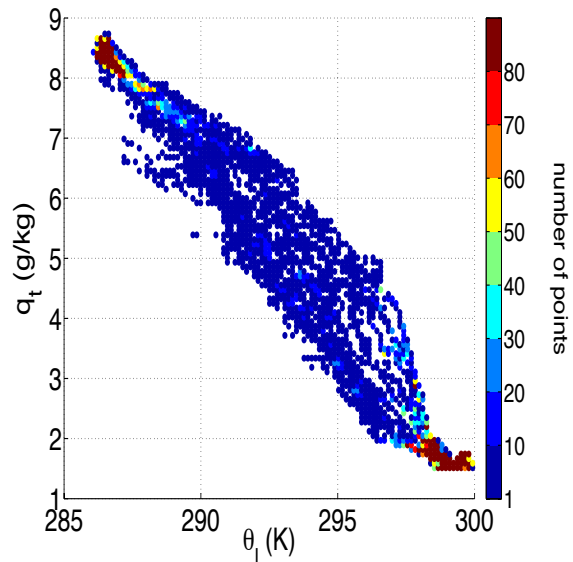
Figure 3: Mixing line from one pod of a daytime flight, when the aircraft was porpoising in and out of the cloudy mixed layer.

4. MIXING FRACTION

The conserved variables q_t and Θ_l were used to calculate a third conserved quantity, mixing
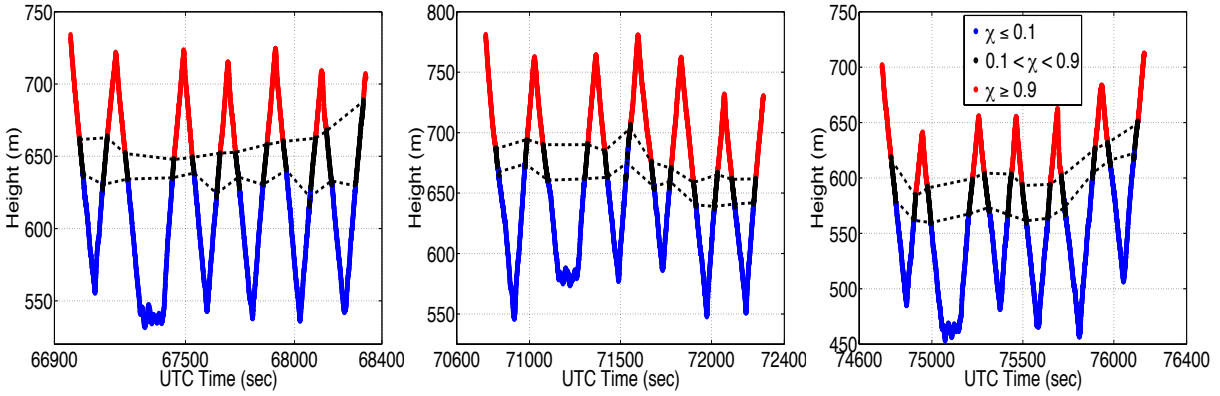
Figure 4: Flightpath characterized by mixing fraction. Black points are characteristic of a layer of mixing between the overlying free atmosphere (red points) and the underlying cloudy mixed layer (blue points).

fraction, for each point along the flight path.

In this case, mixing fraction is defined to be the fractional amount of free-tropospheric air mixed into a parcel of pure cloudy mixed-layer air. Values of mixing fraction range between 0 and 1, with a mixing fraction of 0 meaning no free-tropospheric air has been mixed into the parcel of cloudy air, and therefore representing a parcel of completely pure cloud-layer air. Conversely, a mixing fraction of 1 represents a parcel comprised completely of free-tropospheric air.

Following the methodology of vanZanten and Duynkerke (2002), mixing fraction was computed using the following equation:

$$\chi = \frac{\delta q_t}{\Delta q_t} \quad (2)$$

where

$$\delta q_t = q_{tm} - \overline{q_{t2}}, \quad (3)$$

and

$$\Delta q_t = \overline{q_{t1}} - \overline{q_{t2}}. \quad (4)$$

In the equations above, q_t represents total water mixing ratio, a subscript of 1 represents a pure free-tropospheric value, a subscript of 2 represents a pure cloudy mixed-layer value, a subscript m refers to the mixed parcel, and an overbar indicates an average over the given layer (cloudy

mixed layer or free troposphere). In general, Δq_t is the jump in total water mixing ratio across the inversion at cloud top, and δq_t is the local fluctuation in total water mixing ratio.

Calculating mixing fraction for each point along the porpoising sections of the flightpath allowed for the region near the top of the mixed layer to be plotted in a new way, now characterized by mixing fraction. Values with a mixing fraction of at least 0.9 were taken to be values characteristic of pure free-tropospheric air, and were plotted in red; values with a mixing fraction of 0.1 or less were taken to be characteristic of pure cloud layer air, and were plotted in blue; finally, points with mixing fraction values between those two extremes were taken to be characteristic of parcels in the midst of mixing processes, and were plotted in black. The result, for all flights analyzed, was a clearly defined layer of black points, bordered on the top by red points (the free troposphere), and on the bottom by blue points (the cloudy mixed layer). This result indicates a relatively clearly defined layer of mixing between two pure states of the atmosphere, and is our best approximation for the location and extent of the EIL during POST. Three pods of a daytime flight from POST, characterized by mixing fraction, are shown in Figure 4.

5. EIL RESULTS

To calculate EIL thickness over the course of a flight, the EIL bottom height was subtracted from the EIL top height for each porpoise within the pods of each flight. Those thicknesses were then averaged over all pods within a given flight to produce our best estimate of EIL thickness over an entire flight. Averages of EIL thickness for each of the five analyzed flights are given in Table 1.

For all five flights, individual instances of EIL thickness of several tens of meters were most common. While there were a few instances of extremely thick EILs, they were much less common, and there was only one instance of an especially thin EIL under 10 meters using our mixing fraction technique for defining the EIL.

Table 1: Flight averages of EIL thickness for RF10, RF11, RF12, RF14, and RF16.

Flight	Avg. EIL Thickness (m)
RF10 (daytime)	31.8
RF11 (evening)	43.8
RF12 (evening)	47.0
RF14 (evening)	76.2
RF16 (daytime)	82.5

6. EFFECTS OF RADIATION AND PHASE CHANGES

Relative contributions of radiation and phase changes to a net heating or cooling within the EIL was calculated from moist conserved variables and our new variable, mixing fraction. To calculate the cooling within the EIL due to radiation, we again followed the methodology from vanZanten and Duynkerke (2002):

$$(\delta\Theta_l)_{rad} = \delta\Theta_l - \chi\Delta\Theta_l \qquad (5)$$

where, as with mixing fraction, a subscript of 1 indicates a free troposphere value, a subscript of 2 indicates a cloud layer value, m refers to the mixed parcel, and an overbar indicates an average over the given layer.

$$\delta\Theta_l = \Theta_{lm} - \overline{\Theta_{l2}} \qquad (6)$$

is the local fluctuation in liquid water potential temperature, and

$$\Delta\Theta_l = \overline{\Theta_{l1}} - \overline{\Theta_{l2}} \qquad (7)$$

is the jump in liquid water potential temperature across the inversion at cloud top.

The calculation of cooling/warming within the EIL due to phase changes was accomplished using the following equation, also from vanZanten and Duynkerke (2002):

$$(\Theta_v)_{phase} = (\frac{L_v}{c_{pd}} - 1.61\overline{\Theta_{l2}})(q_{lm} - [1-\chi]\overline{q_{l2}}) \qquad (8)$$

where L_v is the latent heat of vaporization, c_{pd} is the specific heat of dry air at constant pressure, χ is mixing fraction, and the definitions of subscripts and overbars remain the same as for previous equations. In this equation, however, an estimate of the average liquid water mixing ratio of pure cloudy mixed-layer air is required ($\overline{q_{l2}}$). To make a reliable approximation for this quantity, a saturation adjustment code was used, with inputs of pressure, temperature, and vapor mixing ratio from the aircraft data. The code calculated a saturation adjusted value for each point along the flightpath, which were used in the above equation to calculate the relative contribution of phase changes to net heating or cooling within the EIL.

Next, maximum, minimum, and mean values of warming and cooling for binned values of mixing fraction were calculated for temperature effects due to both radiation and phase changes. For these calculations, mixing fraction values were binned over all mixing fractions found within the EIL (0.1-0.9), with a bin width of $\Delta\chi = 0.1$. Mean $(\delta\Theta_l)_{rad}$ and $(\delta\Theta_v)_{phase}$ values were then calculated for each bin, and plotted as a function of mixing fraction, revealing a profile of the effects of radiation and phase changes across the EIL. Plots of these profiles, as well as temperature effects due to mixing, for (a) a daytime flight, and (b) an evening flight are shown in Figure 5.

For daytime RF10, on average, net warming due to radiation occurs in the EIL across all mixing
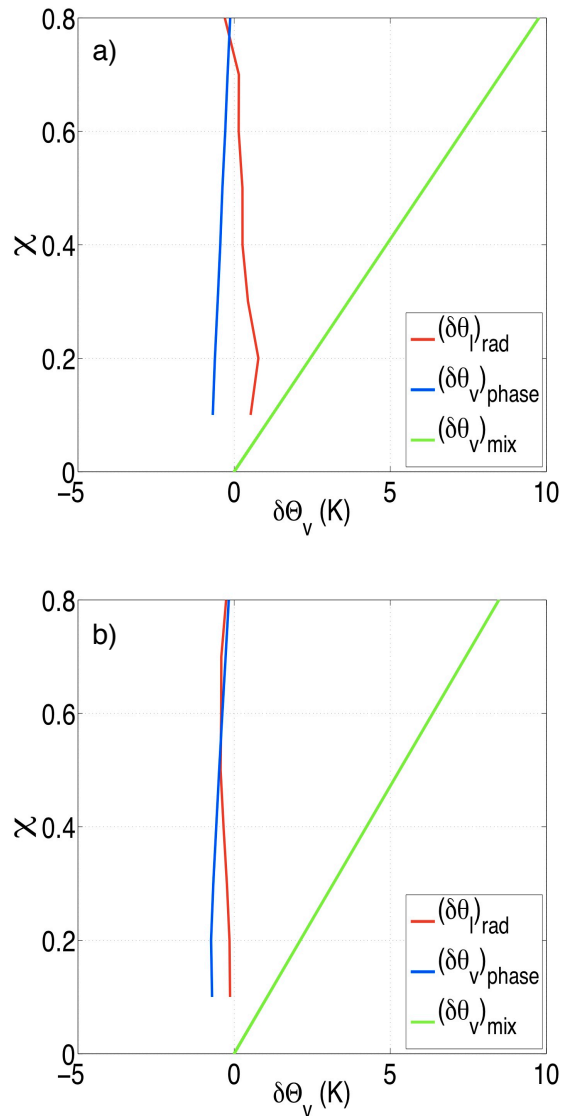
Figure 5: Effects of radiation and phase changes for mixing fractions within the EIL for (a) RF10, a daytime flight, and (b) RF12, an evening flight.

For all analyzed flights, magnitudes of heating and cooling in the EIL due to radiative effects and due to phase changes are comparable, on average. However, as expected, the effects of mixing on heating and cooling within the EIL are much more substantial than those due to radiation or phase changes.

Based on our calculations of mixing fraction, we find a well-defined, substantial EIL between the cloudy mixed layer and the free troposphere for all flights analyzed. Within this EIL, the effects of radiation and phase changes on net heating or cooling near cloud top are of comparable magnitude. These results support the idea that there exists a region between the free troposphere and the cloudy mixed layer of STBLs that has properties intermediate between those of the overlying atmosphere and those of the boundary layer. Our intermediate values of mixing fraction located at altitudes in between the altitude of the free troposphere and the altitude of the boundary layer suggest that this region is also one containing parcels at different stages in the mixing process.

fractions. Evening RF12 exhibits slight cooling due to radiation in the EIL on average, on the same order of magnitude.

Daytime RF10, as well as evening RF12, exhibit net cooling due to phase changes within the EIL across all mixing fraction values, on average. This highlights the effects of evaporative cooling near the top of the cloudy mixed layer, and within the EIL, regardless of the time of day.

REFERENCES

Bony, S., et al., 2006: How well do we understand and evaluate climate change feedback processes? *J. Climate*, **19** (**15**), 3445–3482.

Bretherton, C.S., 1997: Convection in stratocumulus-capped atmospheric boundary layers. In *The Physics and Parameterization of Moist Atmospheric Convection*, R.K. Smith, ed., Klumer Publishers, 127–142 (peer-reviewed book chapter).

Burnet, F. and J.-L. Brenguier, 2007: Observational study of the entrainment-mixing

process in warm convective clouds. *J. Atmos. Sci*, **64**, 1995–2011.

Hartmann, D. L, M. E. Ockert-Bell, and M. L. Michelsen, 1992: The effect of cloud type on earth's energy balance - global analysis. *J. Climate*, **5**, 1281–1304.

Klein, S. A. and D. L. Hartmann, 1993: The seasonal cycle of low stratiform clouds. *J. Climate*, **6**, 1588–1606.

Paluch, I.R., 1979: The entrainment mechanism in Colorado cumuli. **36**, 2467–2478.

vanZanten, M. C., and P.G. Duynkerke, 2002: Radiative and evaporative cooling in the entrainment zone of stratocumulus - the role of longwave radiative cooling above cloud top. *Bound.-Layer Meteor.*, **102**, 253–280.

Wyant, M.C., C.S. Bretherton, J.T. Bacmeister, J.T. Jiehl, I. M. Held, M. Zhao, S. A. Klein, and B.A. Soden, 2006: A comparison of tropical cloud properties and responses in GCMs using mid-tropospheric vertical velocity. *Climate Dyn.*, **27**, 261–279.